VOLUME 17, N° 4 2023
Journal of Automation, Mobile Robotics and Intelligent Systems

Extended State Observer Based Robust Feedback Linearization Control Applied to an Industrial CSTR

Submitted: 25th September 2022; accepted: 27th February 2023

Ali Medjebouri

DOI: 10.14313/JAMRIS/4-2023/32

Abstract:
In the chemical and petrochemical industry, the Continuous Stirred Tank Reactors (CSTR) are, without doubt, one of the most popular processes. From a control point of view, the mathematical model describing the temporal evolution of the CSTR has a strongly nonlinear cross-coupled character. Moreover, modeling errors such as external disturbances, neglected dynamics, and parameter variations or uncertainties make its control task a very difficult challenge. Even though this problem has been the subject of a wide number of control strategies, this article attempts to propose a viable, robust, nonlinear decoupling control scheme. The idea behind the proposed approach lies in the design of two nested control loops. The inner loop is responsible for the compensation of the nominal model nonlinear cross-coupled terms via static nonlinear feedback; whereas the outer loop, designed around an Extended State Observer (ESO) of which the additional state gathers the global effect of modeling errors, is charged to instantaneously estimate, and then to compensate the ESO extended state. This way, the CSTR complex dynamics are reduced to a series of decoupled linear subsystems easily controllable using a simple Proportional-Integral (PI) linear control to ensure the robust pursuit of reference signals respecting the desired performance. The presented control validation was performed numerically by an objective comparison to a classical PID controller. The obtained results clearly show the viability and the effectiveness of the proposed control strategy for dealing with such nonlinear, strongly cross-coupled plants subject to a wide range of disturbances despite the precision of their described mathematical model.

Keywords: *CSTR, Robust control, Feedback Linearization, ESO*

1. Introduction

The CSTR is one of the most used pieces of equipment in process engineering. Its main role is to convert reactants into finished or semi-finished products; therefore, it plays a primary role in many chemical processes [1–4]. CSTRs are generally controlled around a certain equilibrium point, where it is approximated by a locally valid linear model. This approach has the advantage of simplifying the synthesis of the controllers because it allows the use of all classical linear control theory tools.

One of the examples of these classical tools is the PID controller widely used in industrial applications [5–7].

Unrivaled since it appeared in 1922 [8], the PID controller has dominated the industrial scene all over the past century, allowing the propulsion of the technological revolution toward new horizons even in its simple form. The huge success of PID control in the practitioner's society lies essentially in the simplicity of the design and implantation tasks. Nevertheless, pressed by modern industry demands increasingly more and more exigent in terms of efficiency, control theory was always constrained to develop new control mechanisms satisfying the newly imposed requirements [9, 10]. In search of new advanced control schemes, theories have evolved in several directions, giving a very rich bibliography over 80 years.

For the CSTR control example, various control strategies, such as the exact feedback linearization control [11, 12], the nonlinear backstepping control [2], the model predictive control [4, 13–19], different optimal control strategies [20–23], the adaptive control approaches [24–27], and the sliding mode control theory [1, 28–32] have been proposed among others. We can also find several articles based on successful combinations between advanced nonlinear control theories and soft computing tools such as artificial neural networks (ANN) [33, 34], fuzzy inference systems (FIS) [3, 35], and many bio-inspired optimization algorithms such as the genetic algorithm (GA) [7, 36], etc. These combinations have been addressed, in general, to overcome some specific difficulties related to certain synthetic difficulties induced by the mathematical rigor of the original approaches, or to alleviate some disadvantages presented by the previously cited controls.

However, in the midst of this theoretical revolution in the control field, the industry seems uninterested in most of the proposed modern control approaches by presenting a high inflexibility for PID control, even knowing its shortcomings well, despite the improvements introduced to it during the past decades. This fact, probably, lies in their pragmatic way of reflection, aiming most of the time to achieve a sufficiently acceptable compromise between the controller design simplicity and the required performance. On the other hand, it seems that they are missing out on the opportunities offered by the great digital revolution as they cannot fully take profit from the modern digital processor's capacities [9, 10].

Born as a necessity to establish new bridges between modern industry demands and modern control advances, the Active Disturbance Rejection Control (ADRC) was introduced for the first time in the original text in [37] and a few years later for the Anglophone society in [38]. It was the fruit of much work fed by a deep comprehension of both practitioners' and academic researchers' way of reflecting when it comes to addressing control systems problems, the constraints and the challenges facing them, and the opportunities offered by the accelerated development of digital technology.

Even the ADRC original framework is composed from five main components; the Extended State Observer (ESO) represents the controller's cornerstone. The ADRC idea is based on the real time estimation and the active compensation of the total influence of the model nonlinearities combined with the different disturbance types, such as external disturbances, modeling errors, parameters variations or uncertainties, etc. The global effect of the model nonlinearities and disturbances is considered as the observer's augmented state.

Owing to its great potential for dealing with a wide range of disturbance structures, ESO based robust control, including the ADRC original version, has presented an unmistakable viability to address a large set of practical control applications before even having a rigorous proof of theoretical fundamental questions such as the ESO convergence or the closed loop stability which came several years later [39–43]. Moreover, it has shown a high flexibility to handle many more applications than PID control, such as time delayed systems control, multivariable decoupled control, cascade control, and parallel system control [10]. Also, ESO based control has known some major advances in the context of its generalization to more complex problems in the last few past years, such as stochastic systems control [44] and distributed parameter control systems [43].

Motivated by the huge potential, the simplicity of the design procedure, and the wide immergence of ESO based robust control paradigm in simulation and engineering applications, readers can refer to the literature [45–49]. In this paper, we attempt to illustrate how to use the ESO for improving the nonlinear multivariable decoupled control robustness in a simple and clear manner. The proposed method's main idea lies in the use of conventional exact feedback linearization control, widely used for dealing with multivariable affine nonlinear plants in association with an extended state observer charged to estimate in real-time and then actively compensate the whole effect of modeling errors caused by the total difference between the real plant dynamics and the nominal descriptive model used for the design of the decoupling static state feedback. The desired, robust closed loop dynamics are achieved using a proportional-integral controller in a second external loop.

The present article is organized as follows: After presenting this introduction, the second section is devoted to the process presentation and modeling. Then, the theoretical development of the proposed control is exposed in detail. Once the process model and the controller design are presented, the simulation results are shown and commented on in the third section. Finally, the conclusion summarizing and highlighting main advantages of the proposed control strategy is given in the fourth and last section.

2. The CSTR Mathematical Model

The proposed CSTR model, shown in Figure 1, is described by the equations given below as found in [50]:

$$\begin{cases} \dfrac{dC_A}{dt} = \dfrac{1}{V}\Delta F_L(C_{Ai} - C_A) - k_0 \exp\left(\dfrac{-E_a}{RT_R}\right) C_A \\ \dfrac{dT_R}{dt} = \dfrac{1}{V}\Delta F_C(T_i - T_R) - \dfrac{\Delta H.k_0}{\rho.C} \exp\left(\dfrac{-E_a}{RT_R}\right) C_A \\ \qquad + \dfrac{U.A}{V.\rho.C}(T_C - T_R) \end{cases} \tag{1}$$

It is obvious that the model (1) is of the form:

$$\begin{cases} \dot{x} = F(x) + G(x)u \\ \quad y = h(x) \end{cases} \tag{2}$$

where:

- $x = \begin{bmatrix} x_1 & x_2 \end{bmatrix}^T = \begin{bmatrix} C_A & T_R \end{bmatrix}^T$: is the state vector.
- $u = \begin{bmatrix} u_1 & u_2 \end{bmatrix}^T = \begin{bmatrix} F_L & F_C \end{bmatrix}^T$: the control input.
- $y = h(x) = x$: the controlled output.

$$F(x) = \begin{bmatrix} -k_0 \exp\left(\dfrac{-E_a}{Rx_2}\right) x_1 \\ -\dfrac{\Delta H.k_0}{\rho.C} \exp\left(\dfrac{-E_a}{Rx_2}\right) x_1 + \dfrac{U.A}{V.\rho.C}(T_i - x_2) \end{bmatrix} \tag{3}$$

$$G(x) = \begin{bmatrix} \dfrac{1}{V}(C_{Ai} - x_1) & 0 \\ 0 & \dfrac{1}{V}(T_i - x_2) \end{bmatrix} \tag{4}$$

Control inputs, controlled outputs, and process parameters are given in Table 1.

3. Feedback Linearization Control

The necessary and sufficient condition allowing the existence of static, nonlinear feedback ensuring the exact linearization of the system (2) is guaranteed if and only if the output's global relative degree equals to the system's order.

Table 1. Proposed CSTR manipulated variables and parameters [50]

Symbol	Description	Value
F_L	Reactant fluid flow rate [m³/h]	–
F_C	Coolant fluid flow rate [m³/h]	–
C_A	Concentration of the reactant A in the reactor [kg mol/ m³]	–
T_R	Temperature in the CSTR [K]	–
V	Reaction volume [m³]	24
A	Effective heat interchange surface [m²]	24
ΔH	Enthalpy of the reaction [kJ/kmol]	−2100
E_a	activation energy [kJ/kmol]	2100
k_0	Reaction velocity constant [h⁻¹]	59,063
ρ	Density of the reactant A [kg/ m³]	800
U	Heat transfer coefficient between the cooling jacket and the reactor [kJ/(h. m³.K)]	4300
T_i	Jacket cooling fluid initial temperature [K]	306
C_{Ai}	Feed concentration of reactant A[kg mol/ m³]	10
C	Specific heat capacity of reactant A [kJ/(kg.K)]	3
R	Ideal gas constant [kJ/kg kmol]	8,314

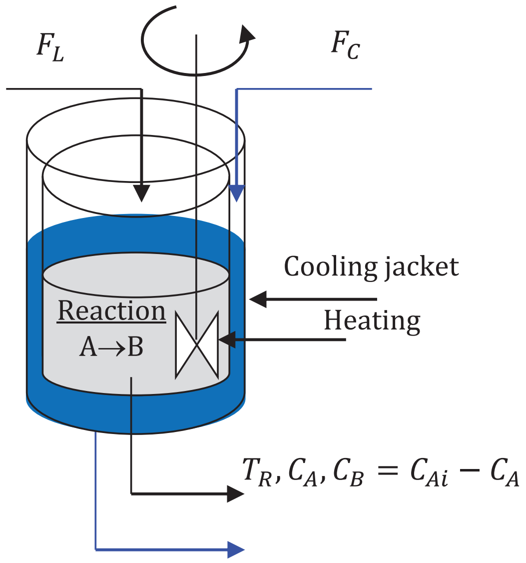

Figure 1. Simplified scheme of the proposed CSTR

3.1. The Output Relative Degree

By definition, the output relative degree is the least number of the output's time derivatives to get at least one control input [51]:

$$\dot{y} = \begin{bmatrix} \dot{h}_1(x) \\ \dot{h}_2(x) \end{bmatrix} = \begin{bmatrix} L_F h_1(x) + L_G h_1(x).u \\ L_F h_2(x) + L_G h_2(x).u \end{bmatrix}$$

$$= \begin{bmatrix} -k_0 \exp\left(\frac{-E_a}{Rx_2}\right) x_1 + \frac{1}{V}(C_{Ai} - x_1)\, u_1 \\ -\frac{\Delta H.k_0}{\rho.C} \exp\left(\frac{-E_a}{Rx_2}\right) x_1 + \frac{U.A}{V.\rho.C}(T_i - x_2) \\ + \frac{1}{V}(T_i - x_2) u_2 \end{bmatrix} \quad (5)$$

From (5), it is clear that C_A and T_R relative degrees are equal respectively to $r_1 = 1$ and $r_2 = 1$.

Therefore, the output vector global relative degree is equal to $r = r_1 + r_2 = 2$, and noting that the system order $n = 2$, the existence of a static nonlinear feedback allowing the exact linearization of (2) is then ensured.

Equation (5) can be rewritten as described below:

$$\dot{y} = \begin{bmatrix} \dot{h}_1(x) \\ \dot{h}_2(x) \end{bmatrix} = A(x) + D(x).u \quad (6)$$

where:

$$A(x) = \begin{bmatrix} L_F h_1(x) \\ L_F h_2(x) \end{bmatrix} = F(x) \quad (7)$$

$$D(x) = \begin{bmatrix} L_G h_1(x) \\ L_G h_2(x) \end{bmatrix} = G(x) \quad (8)$$

L_F, L_G denotes the Lie derivatives [51].

3.2. Linearizing Feedback Control Design

From the equation (5), it is obvious that the searched static nonlinear feedback linearization control is defined as:

$$u = D^{-1}(x).[V - A(x)] \quad (9)$$

where, $A(x)$ and $D(x)$ are given by the equations (3) and (4) respectively. The term $V = [v_1\ v_2]^T$ is the new control input issued from the external control loop.

Applying the control law (9) to the system (2) leads to the following linear decoupled system:

$$\begin{cases} \dot{x}_1 = v_1 \\ \dot{x}_2 = v_2 \end{cases} \quad (10)$$

3.3. Outer Loop Controller Synthesis

Applying the following PI control law to the outer control loop:

$$\begin{cases} v_1 = -K_{11} C_A - K_{12} \int (C_A - C_A^{ref}) dt \\ v_2 = -K_{21} T_R - K_{22} \int (T_R - T_R^{ref}) dt \end{cases} \quad (11)$$

yields the following closed loop transfer function:

$$G(s) = \begin{bmatrix} \frac{K_{12}}{s^2 + K_{11}s + K_{12}} & 0 \\ 0 & \frac{K_{22}}{s^2 + K_{21}s + K_{22}} \end{bmatrix}$$

$$= \begin{bmatrix} \frac{\omega_1^2}{s^2 + 2\zeta_1\omega_1 s + \omega_1^2} & 0 \\ 0 & \frac{\omega_2^2}{s^2 + 2\zeta_2\omega_2 s + \omega_2^2} \end{bmatrix} \quad (12)$$

where, s is the Laplace operator, ζ_i and ω_i are respectively the closed loop desired damping ratios and band-width frequencies.

3.4. Extended State Observer Based Robust Feedback Linearization Control

First, let us introduce the modeling errors by considering them as parameters variations and uncertainties in the nominal model (2). This leads to the following perturbed model:

$$\begin{cases} \dot{x} = F(x) + \Delta F(x) + (G(x) + \Delta G(x))u \\ y = h(x) \end{cases} \tag{13}$$

By applying the nonlinear control feedback (9) to the perturbed system (13), the exactly linearized system (10) becomes of the form:

$$\dot{x} = V + \eta(x, V) \tag{14}$$

where:

$$\eta(x, V) = \Delta G(x) G^{-1}(x)(V - F(x)) + \Delta F(x) \tag{15}$$

The system (14) can be re-expressed as:

$$\begin{cases} \dot{x}_1 = v_1 + \eta_1(x, V) \\ \dot{x}_2 = v_2 + \eta_2(x, V) \end{cases} \tag{16}$$

The next step consists of designing two extended state observers, allowing the estimation of the system states and the two unknown disturbances functions η_1 and η_2. So, each subsystem of equation (16) can be rewritten in the following state form:

$$\begin{cases} \dot{x}_{i1} = x_{i2} + v_i \\ \dot{x}_{i2} = \dot{\eta}_i \end{cases} \quad i = 1, 2 \tag{17}$$

The proposed nonlinear extended states observers (NLESO) are defined as given in [41]:

$$\begin{cases} \dot{\hat{x}}_i = A.\hat{x}_i + B.v_i + L_i.g_i(\hat{e}_i) \\ \hat{y}_i = \hat{x}_{i1} \end{cases} \tag{18}$$

where:

$$A = \begin{bmatrix} 0 & 1 \\ 0 & 0 \end{bmatrix}, B = \begin{bmatrix} \mathrm{b} \\ 0 \end{bmatrix}, \hat{x}_i = \begin{bmatrix} \hat{x}_{i1} \\ \hat{x}_{i2} \end{bmatrix}, L_i = \begin{bmatrix} L_{i1} \\ L_{i2} \end{bmatrix} \tag{19}$$

The nonlinear $g(e_i)$ function is defined as:

$$g_i(\hat{e}_i) = \begin{cases} |\hat{e}_i|^{\alpha_i}.sign(\hat{e}_i) & , if\ |\hat{e}_i| > \delta_i \\ \dfrac{\hat{e}_i}{\delta_{\mathrm{i}}^{1-\alpha_i}}, & else \end{cases} \quad i = 1, 2 \tag{20}$$

where:

$$0 < \alpha_i < 1, \delta_i > 0, \hat{e}_i = y_i - \hat{y}_i \tag{21}$$

when $|\hat{e}_i| < \delta_i$, the nonlinear state observer (18) takes the form of the well known linear Luenberger observer (LESO):

$$\begin{cases} \dot{\hat{x}}_{i1} = \hat{x}_{i2} + \beta_{i1}\hat{e}_i + v_i \\ \dot{\hat{x}}_{i2} = \beta_{i2}\hat{e}_i \end{cases}, \beta_{ij} = \frac{L_{ij}}{\delta^{1-\alpha_i}} i, j = 1, 2 \tag{22}$$

Therefore, β_i are calculated to ensure an observer dynamic faster than the close loop tracking dynamic as described by the given below condition:

$$P_{LESO}(s) = s^2 + \beta_{i2}s + \beta_{i1} = (s + \omega_{i0})^2 \tag{23}$$

$P_{LESO}(s)$: The observer's characteristic polynomial.
ω_{i0}: The desired observer band-width frequency.
ω_{i0}: Is chosen as given in [52] to ensure the best compromise between the observing convergence speed and the sensors noise insensitivity:

$$\omega_{i0} = (3 \text{ to } 5)\omega_i, i = 1, 2 \tag{24}$$

The small value δ_i represents the set point limiting the NLESO (18) high gain.

By redefining the outer loop control (11) as follows:

$$\begin{cases} v_1^{Rob} = v_1 + \Delta v_1 \\ v_2^{Rob} = v_2 + \Delta v_2 \end{cases} \tag{25}$$

where:

$$\begin{cases} \Delta v_1 = -\hat{x}_{12} \\ \Delta v_2 = -\hat{x}_{22} \end{cases} \tag{26}$$

the controlled outputs in presence of modeling errors computed in the Laplace domain become:

$$\begin{cases} C_A(\mathrm{s}) = \dfrac{\omega_1^2}{s^2 + 2\zeta_1\omega_1 s + \omega_1^2} C_A^{ref}(\mathrm{s}) \\ + \dfrac{1}{s^2 + 2\zeta_1\omega_1 s + \omega_1^2}(\eta_1(s) - \hat{X}_{12}(s)) \\ T_R(\mathrm{s}) = \dfrac{\omega_2^2}{s^2 + 2\zeta_2\omega_2 s + \omega_2^2} T_R^{ref}(\mathrm{s}) \\ + \dfrac{1}{s^2 + 2\zeta_2\omega_2 s + \omega_2^2}(\eta_2(s) - \hat{X}_{22}(s)) \end{cases} \tag{27}$$

It is obvious that when the estimated states converge to the system states:

$$\begin{cases} \eta_1(s) \to \hat{X}_{12}(s) \\ \eta_2(s) \to \hat{X}_{22}(s) \end{cases} \tag{28}$$

the controlled outputs dynamics converge to the given below expressions:

$$\begin{cases} C_A(\mathrm{s}) \cong \dfrac{\omega_1^2}{s^2 + 2\zeta_1\omega_1 s + \omega_1^2} C_A^{ref}(\mathrm{s}) \\ T_R(\mathrm{s}) \cong \dfrac{\omega_2^2}{s^2 + 2\zeta_2\omega_2 s + \omega_2^2} T_R^{ref}(\mathrm{s}) \end{cases} \tag{29}$$

It is clear from (29) that the closed loop dynamic and static desired performances are guaranteed. However, we shall emphasize that the analytical convergence proof of the NLESO (18) is out of the scope of this paper, and we are limited just to suppose the assumptions given in [42, p. 421] are satisfied and the validity of the proposed control is demonstrated through numerical simulations.

4. Simulation Results and Discussion

The proposed control method is validated using numerical simulations by comparing it objectively to the conventional PI controller designed basing on a locally valid linear model developed around a preselected operating point. The conventional PI synthesis method is given bellow choosing the following operating state:

$$x_0 = \begin{bmatrix} 2.88 & 297 \end{bmatrix}^T \quad u_0 = \begin{bmatrix} 244.96 & 212.56 \end{bmatrix}^T$$

Hence, the linear state model is given by the following matrices:

$$A_0 = \begin{bmatrix} -35.44 & -61.80 \\ -22.08 & -7.25 \end{bmatrix};\ B_0 = \begin{bmatrix} 0.30 & 0 \\ 0 & 0.38 \end{bmatrix}$$

$$C_0 = \begin{bmatrix} 1 & 0 \\ 0 & 1 \end{bmatrix};\ D_0 = \begin{bmatrix} 0 & 0 \\ 0 & 0 \end{bmatrix}$$

Notice that the local behavior of the given above model is unstable at the chosen operating point. The calculation of the matrix A_0 eigenvalues yields:

$$\lambda(A_0) = \begin{bmatrix} -60.88 & 18.19 \end{bmatrix}^T$$

To introduce the integral action in the control law using state feedback closed loop pole placement method, let us consider the following augmented system: where the augmented state is defined as:

$$x = \begin{bmatrix} C_A & T_R & e_1 = C_A - C_A^{ref} & e_2 = T_R - T_R^{ref} \end{bmatrix}^T$$

Choosing the closed loop poles as follows:

$$\lambda(A_C) = \begin{bmatrix} -61 & -20 & -61 & -20 \end{bmatrix}^T$$

the closed loop PI controller is described by the following equations:

$$u = u_0 + \Delta u$$

where:

$$\Delta u = K_P \begin{bmatrix} C_A \\ T_R \end{bmatrix} + K_I \int \begin{bmatrix} (C_A - C_A^{ref}) \\ (T_R - T_R^{ref}) \end{bmatrix} dt$$

$$K_P = 10^3 \begin{bmatrix} 0.15 & -0.21 \\ -0.06 & 0.20 \end{bmatrix}\ K_I = 10^3 \begin{bmatrix} 4.11 & 0 \\ 0 & 3.25 \end{bmatrix}$$

The comparative study that follows is based on two scenarios:

<u>**Scenario 1:**</u> Both proposed controls are applied to the nominal nonlinear model of which the parameters are given in Table 1.

The proposed ESO based robust controller parameters are defined as given in Table 2.

<u>**Scenario 2:**</u> The compared controllers are applied to the uncertain model in order to test their performance robustness against parameter's, uncertainties, and variations of parameters are given in table below:

The proposed ESO based robust feedback linearization control bloc scheme and the obtained simulation results for each proposed scenario are presented in Figures 2–16.

Table 2. ESO based controllers' parameters

Loop	Controller/ESO parameters
C_a	$\zeta_1 = 1;\ \omega_1 = 61;$ $\omega_{10} = 183;\ \delta_1 = 0.1;\ \alpha_{11} = 0.5;\ \alpha_{12} = 0.05$
T_R	$\zeta_2 = 1;\ \omega_2 = 20;$ $\omega_{20} = 100;\ \delta_2 = 10^{-5};\ \alpha_{21} = 0.495;\ \alpha_{21} = 0.005$

Table 3. Parameters uncertainties or variations

Uncertainties/ variations	Absolute value	Relative value (%)
$\Delta V(t)$	0,25x24.sin(t)	[−25 +25]
$\Delta A(t)$	0,25x24.sin(t)	[−25 +25]
$\Delta C_{Ai}(t)$	0,2x10.sin(t)	[−20 +20]
$\Delta T_i(t)$	0,02x306.sin(t)	[−2 +2]
$\Delta(\Delta H)$	−0,01.2100	−1
Δk_0	−0,05x59,063	−5
$\Delta\rho$	+0,05x800	+5
ΔU	−0,1x4300	−10
ΔC	+0,01.3	+1
ΔE_a	−0,1x2100	−10

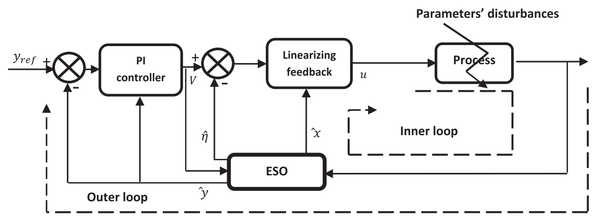

Figure 2. The proposed ESO based robust feedback linearization control scheme

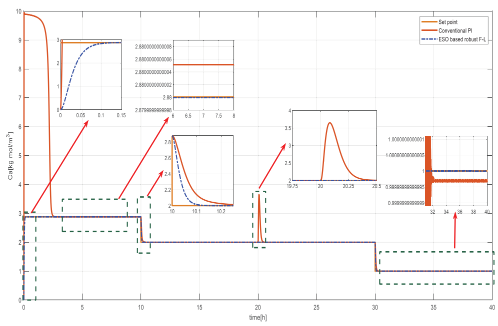

Figure 3. Desired and actual product's concentration curves for scenario 1

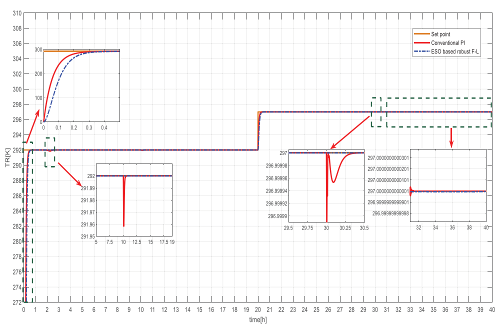

Figure 4. Desired and actual product's temperature curves for scenario 1

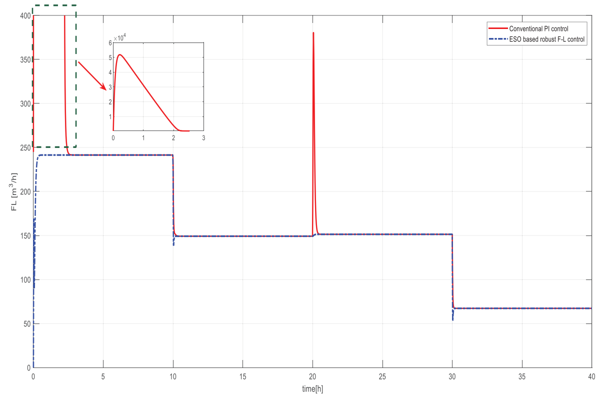

Figure 5. Reactant fluid flow rate control input curves for scenario 1

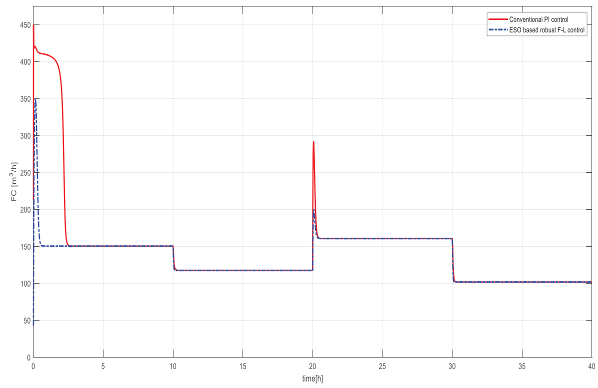

Figure 6. Coolant fluid flow rate control input curves for scenario 1

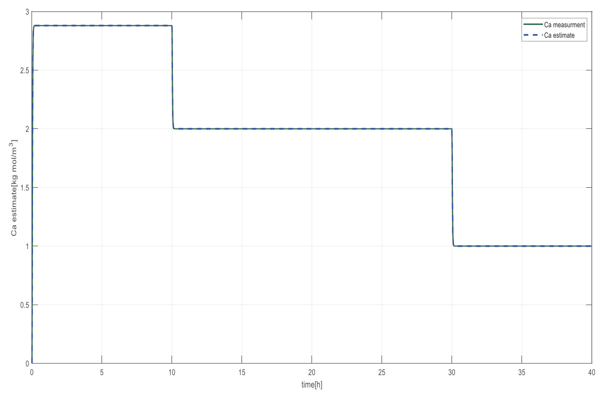

Figure 7. Measured and observed product's concentration curves for scenario 1

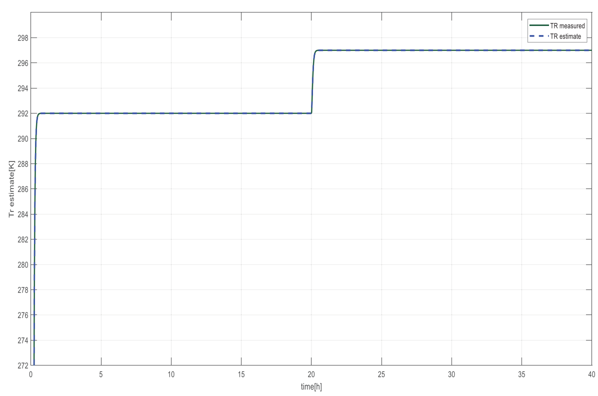

Figure 8. Measured and observed product's temperature curves for scenario 1

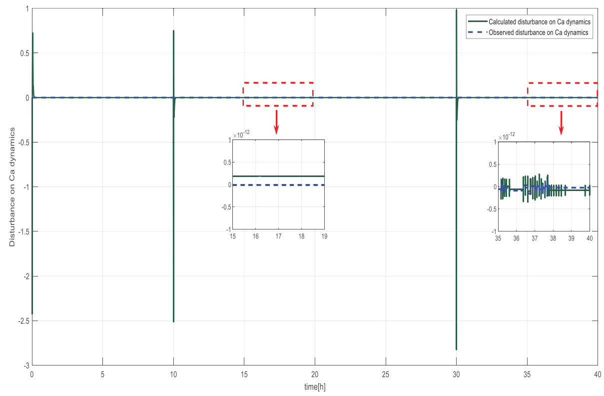

Figure 9. Calculated and observed product's concentration dynamics uncertainties curves for scenario 1

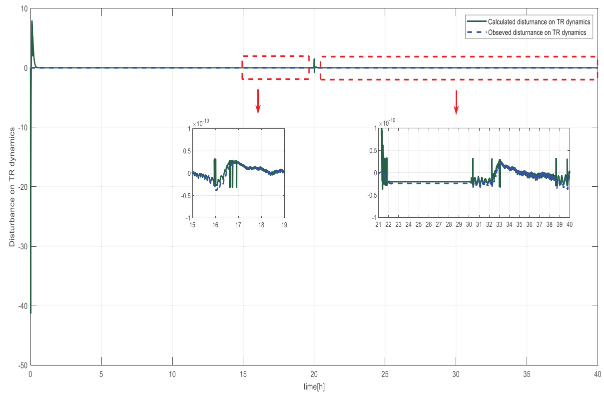

Figure 10. Calculated and observed product's temperature dynamics uncertainties curves for scenario 1

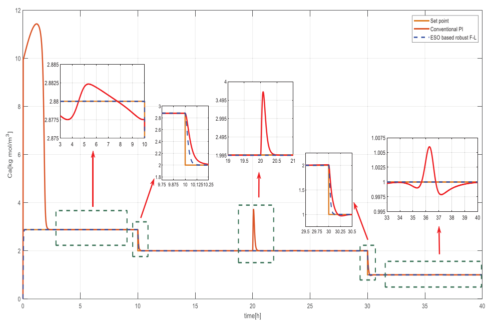

Figure 11. Desired and actual product's concentration curves for scenario 2

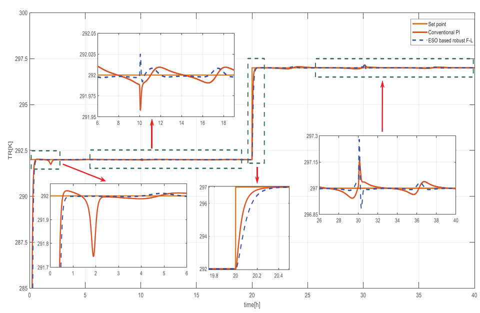

Figure 12. Desired and actual product's temperature curves for scenario 2

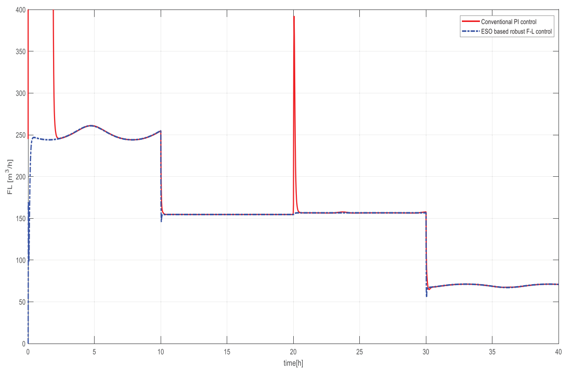

Figure 13. Reactant fluid flow rate control input curves for scenario 2

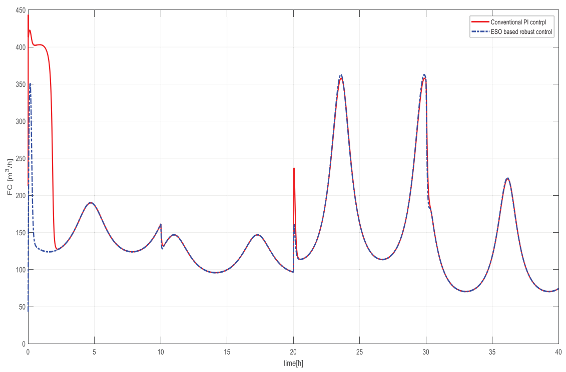

Figure 14. Coolant fluid flow rate control input curves for scenario 2

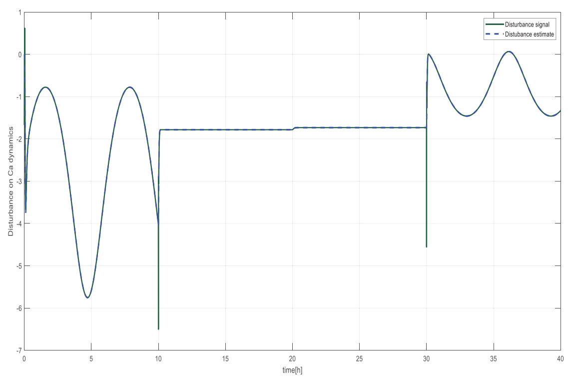

Figure 15. Calculated and observed product's concentration dynamics uncertainties curves for scenario 2

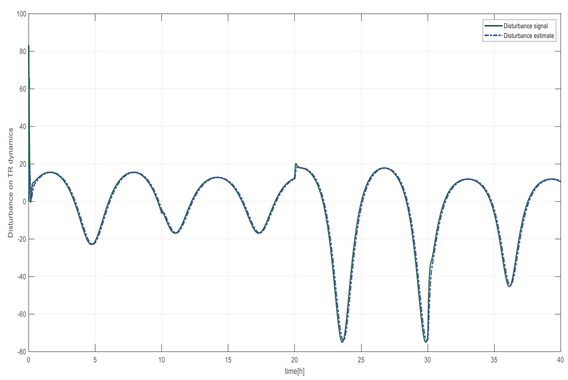

Figure 16. Calculated and observed product's temperature dynamics uncertainties curves for scenario 2

4.1. Results Discussion When the Process is Operating in Nominal Conditions

When the parameters' uncertainties and variations are equal to zero, the responses of the CSTR under the both proposed controllers, shown in the Figures 3 and 4, remain very close to the desired set point after the transient phases. It is also clear in Figure 3 that the ESO based robust feedback linearizing controller ensures a better decoupling between the controlled outputs and a faster convergence of the product concentration to its desired value. The strong inertia of the process against the conventional PI controller disappears after a certain elapsed period of time. Concerning the temperature responses, it clearly illustrated in Figure 4 that the conventional PI control exhibits a slightly superior convergence speed although the chosen closed loop poles were the same. This result is due to the fact that for the conventional PI control, the closed loop temperature dynamics are regulated as a first order subsystem, whereas it is chosen as a second order critically damped subsystem for the ESO based robust controller.

The control signals depicted in Figures 5 and 6 confirm the high inertia of the controlled process against the conventional PI controller by illustrating the high control effort needed to achieve the desired values when the process is started or when the set point changes suddenly, this remark is more evident for the supply control flow FL.

From Figures 9 and 10, it is seen clearly that convergence of the proposed ESO is very satisfactory. The estimate of the total modeling errors supposed unknown and considered as an additional state remain near zero. This expected result is logical since in this scenario the model's uncertainties were neglected by setting their values to zero.

4.2. Results Discussion When the Process is Operating in Presence of Parameters', Uncertainties, or Variations

In scenario 2, our aim was to compare the transient and steady performances of the proposed controllers under the suppositions of the existence of uncertain or time varying parameters. The results presented in Figures 11 and 12 show that even the nominal performances were relatively degraded compared to the nominal case; both proposed controllers were able to achieve sufficiently good control performance in the sense that the system responses were maintained around the desired set points within a narrow band. Also, it is clear that the proposed ESO based robust feedback controller robustness exceeds that obtained with the conventional PI since it was capable of ensuring a better static precision by rejecting actively the real-time observed modeling errors as depicted in Figures 15 and 16.

Table 4. Rooted mean squared error and mean control power criterions for each scenario

		ESO based F-L controller		PI controller	
		C_A	T_R	C_A	T_R
RMS	1	0,103	13,64	1,565	10,87
	2	0,144	19,00	1,721	15,40
		F_L	F_C	F_L	F_C
Mean control power	1	$2{,}68\times10^4$	$1{,}88\times10^4$	$54{,}35\times10^6$	$2{,}60\times10^4$
	2	$2{,}34\times10^4$	$2{,}86\times10^4$	$48{,}27\times10^6$	$2{,}99\times10^4$

In term of control energy, the Figures 13 and 14 highlight the main future of the proposed ESO based robust feedback control, which lies in the fact that it needs a net inferior energetic consumption to achieve the desired set points when these desired values change instantaneously and especially when the process starts functioning. This major feature, clearly visible in Table 4, is due to the potential of the proposed method to decouple the whole process dynamics into two independent dynamics and thus control them separately, dispensing less energy compared to the PI controller.

The above presented comparative study is summarized based on the rooted mean square error and the mean control power criterions for each scenario in Table 4.

The error RMS and the mean control power criterions are defined as:

$$\begin{cases} RMS(e(t)) = \sqrt{\dfrac{1}{T}\displaystyle\int_0^T e^2(t)dt} \\ Mean\ power(u(t)) = \dfrac{1}{T}\displaystyle\int_0^T u^2(t)dt \end{cases} \tag{30}$$

where:
T: is the simulation time.
u(t): represents the control input.

5. Conclusion

The main objective of this article was to propose a viable extended state observer based robust feedback linearization controller applied to the control of an industrial CSTR. The idea behind this particular choice was to associate the decoupling capacity of the exact feedback linearization control, and therefore guaranteeing high tracking performance, and the high potential of the nonlinear extended state observer to estimate the modeling errors and the external disturbances in order to reject actively their undesirable effects. The obtained results via numerical simulations have objectively demonstrated the effectiveness of the proposed control strategy compared to the conventional PI in terms of:

1) Providing a better tracking performance by ensuring a better decoupling between the two controlled dynamics.
2) Presenting a remarkable energetic efficiency improvement by diminishing the power consumption.
3) Showing a strong robustness against the nominal model's uncertainties by decreasing the necessity to get a highly accurate mathematical model in the controller design by adopting an extended state observer charged to compensate the model/plant mismatch.

AUTHOR
Ali Medjebouri* – Department of Mechanical Engineering, University of 20 August 1955, Skikda, 21000, Algeria, e-mail: ali.medjbouri@gmail.com, a.medjebouri@univ-skikda.dz.

*Corresponding author

References

[1] D. Zhao, Q. Zhu, and J. Dubbeldam. "Terminal sliding mode control for continuous stirred tank reactor," *Chemical Engineering Research and Design*, vol. 94, pp. 266–274, Feb. 2015, doi: 10.1016/j.cherd.2014.08.005.

[2] S. Alshamali and M. Zribi. "Backstepping control design for a continuous-stirred tank," *International Journal of Innovative Computing, Information and Control*, vol. 8, pp. 7747–7760, Nov. 2012.

[3] Nasser Mohamed Ramli and Mohamad Syafiq Mohamad. "Modelling for Temperature Non-Isothermal Continuous Stirred Tank Reactor Using Fuzzy Logic", Jan. 2017, doi: 10.5281/zenodo.1128853.

[4] S. Li, X. J. Zong, and Y. Hu. "Model Predictive Control of Continuous Stirred-Tank Reactor," *Advanced Materials Research*, vol. 760–762, pp. 1000–1003, 2013, doi: 10.4028/www.scientific.net/AMR.760-762.1000.

[5] R. Upadhyay and R. Singla. "Analysis of CSTR Temperature Control with Adaptive and PID Controller (A Comparative Study)," *International Journal of Engineering and Technology*, vol. 2, pp. 453–458, Jan. 2010, doi: 10.7763/IJET.2010.V2.164.

[6] M. Saad, A. Albagul, and D. Obaid. "Modeling and Control Design of Continuous Stirred Tank Reactor System," Jan. 2013.

[7] A. Singh and V. Sharma. "Concentration control of CSTR through fractional order PID controller by using soft techniques," in *2013 Fourth*

International Conference on Computing, Communications and Networking Technologies (ICCCNT), Jul. 2013, pp. 1–6. doi: 10.1109/ICCCNT.2013.6726501.

[8] N. Minorsky.. "Directional Stability of Automatically Steered Bodies," *Journal of the American Society for Naval Engineers*, vol. 34, no. 2, pp. 280–309, 1922, doi: 10.1111/j.1559-3584.1922.tb04958.x.

[9] Z. Gao. "Active disturbance rejection control: a paradigm shift in feedback control system design," in *2006 American Control Conference*, Jun. 2006, p. 7. doi: 10.1109/ACC.2006.1656579.

[10] J. Han. "From PID to Active Disturbance Rejection Control," *IEEE Transactions on Industrial Electronics*, vol. 56, no. 3, pp. 900–906, Mar. 2009, doi: 10.1109/TIE.2008.2011621.

[11] C. Kravaris and C.-B. Chung. "Nonlinear State Feedback Synthesis by Global Input/Output Linearization," in *1986 American Control Conference*, Jun. 1986, pp. 997–1005. doi: 10.23919/ACC.1986.4789080.

[12] M. Hajaya and T. Shaqarin. "Control of a Benchmark CSTR Using Feedback Linearization," *JORDANIAN JOURNAL OF ENGINEERING AND CHEMICAL INDUSTRIES (JJECI)*, vol. 2, pp. 67–75, Oct. 2019, doi: 10.48103/jjeci292019.

[13] U. Kumar, V. Sharma, O. P. Rahi, and V. Kumar. "MPC-Based Temperature Control of CSTR Process and Its Comparison with PID," in *Advances in Electrical and Computer Technologies*, T. Sengodan, M. Murugappan, and S. Misra, Eds., in Lecture Notes in Electrical Engineering. Singapore: Springer, 2020, pp. 1109–1115. doi: 10.1007/978-981-15-5558-9_94.

[14] A. M. Deulkar, A. B. Patil. "Temperature control of continuous stirred tank reactor using model predictive controller,"*Proceedings of IT Research International Conference, Kolhapur, India*, 2015, ISBN: 978-93-85465-40-6.

[15] J. Pekaø and V. Havlena. "Control of CSTR using model predictive controller based on mixture distribution," *IFAC Proceedings Volumes*, vol. 37, no. 13, pp. 793–798, Sep. 2004, doi: 10.1016/S1474-6670(17)31322-8.

[16] F. Wu. "LMI-based robust model predictive control and its application to an industrial CSTR problem," *Journal of Process Control*, vol. 11, no. 6, pp. 649–659, Dec. 2001, doi: 10.1016/S0959-1524(00)00052-4.

[17] H. Chen, H. Kremling, and F. Allgöwer. "Nonlinear Predictive Control of a Benchmark CSTR," *Proceedings of the 3rd European Control Conference, Rome-Italy.*, pp. 3247–3252, Jan. 1995.

[18] P. B. Sistu and B. W. Bequette. "Nonlinear predictive control of uncertain processes: Application to a CSTR," *AIChE Journal*, vol. 37, no. 11, pp. 1711–1723, 1991, doi: 10.1002/aic.690371114.

[19] A. Krishnan, B. V. Patil, P. S. V. Nataraj, J. Maciejowski, and K. V. Ling. "Model predictive control of a CSTR: A comparative study among linear and nonlinear model approaches," in *2017 Indian Control Conference (ICC)*, Jan. 2017, pp. 182–187. doi: 10.1109/INDIANCC.2017.7846472.

[20] D. Gao. "Feedback Linearization Optimal Control Approach for Bilinear Systems in CSTR Chemical Reactor," *Intelligent Control and Automation*, vol. 03, pp. 274–277, Jan. 2012, doi: 10.4236/ica.2012.33031.

[21] K. B. Pathak, A. Markana, and N. Parikh. "Optimal Control of CSTR," *Nirma University Journal of Engineering and Technology*, 2000, Available: https://www.semanticscholar.org/paper/Optimal-Control-of-CSTR-Pathak-Markana/f4a41e3ef3b742141cbb58bb2ced4906a056f024.

[22] P. R. Meghna, V. Saranya, and B. J. Pandian. "Design of Linear-Quadratic-Regulator for a CSTR process," *IOP Conf. Ser.: Mater. Sci. Eng.*, vol. 263, no. 5, p. 052013, Nov. 2017, doi: 10.1088/1757-899X/263/5/052013.

[23] D.-X. Gao, H. Liu, and J. Cheng. "Optimal output tracking control for chemical process of non-isothermal CSTR," in *2016 Chinese Control and Decision Conference (CCDC)*, May 2016, pp. 4588–4592. doi: 10.1109/CCDC.2016.7531811.

[24] R. Upadhyay and R. Singla. "Analysis of CSTR Temperature Control with Adaptive and PID Controller (A Comparative Study)," *International Journal of Engineering and Technology*, vol. 2, pp. 453–458, Jan. 2010, doi: 10.7763/IJET.2010.V2.164.

[25] K.-U. Klatt and S. Engell. "Gain-scheduling trajectory control of a continuous stirred tank reactor," *Computers & Chemical Engineering*, vol. 22, no. 4, pp. 491–502, Jan. 1998, doi: 10.1016/S0098-1354(97)00261-5.

[26] R. B. Gopaluni, I. Mizumoto, and S. L. Shah. "A Robust Nonlinear Adaptive Backstepping Controller for a CSTR," *Ind. Eng. Chem. Res.*, vol. 42, no. 20, pp. 4628–4644, Oct. 2003, doi: 10.1021/ie020412b.

[27] D. Stavrov, G. Nadzinski, S. Deskovski, and M. Stankovski. "Quadratic Model-Based Dynamically Updated PID Control of CSTR System with Varying Parameters," *Algorithms*, vol. 14, no. 2, Art. no. 2, Feb. 2021, doi: 10.3390/a14020031.

[28] M. C. Colantonio, A. C. Desages, J. A. Romagnoli, and A. Palazoglu. "Nonlinear Control of a CSTR: Disturbance Rejection Using Sliding Mode Control," *Ind. Eng. Chem. Res.*, vol. 34, no. 7, pp. 2383–2392, Jul. 1995, doi: 10.1021/ie00046a022.

[29] M. Luning, Y. Xiao, Z. Dongya, and S. K. Spurgeon. "Disturbance observer based sliding mode

control for a continuous stirred tank reactor (CSTR)," in *2017 36th Chinese Control Conference (CCC)*, Jul. 2017, pp. 3748–3753. doi: 10.23919/ChiCC.2017.8027943.

[30] J. Feng, L. Ma, D. Zhao, X. Yan, and S. K. Spurgeon. "Output Feedback Sliding Mode Control for Continuous Stirred Tank Reactors," in *2019 12th Asian Control Conference (ASCC)*, Jun. 2019, pp. 1443–1448. Available: https://ieeexplore.ieee.org/abstract/document/8765099.

[31] W. García-Gabín, J. E. Normey-Rico, and Eduardo. F. Camacho. "Sliding Mode Predictive Control of a Delayed CSTR," *IFAC Proceedings Volumes*, vol. 39, no. 10, pp. 246–251, Jan. 2006, doi: 10.3182/20060710-3-IT-4901.00041.

[32] A. Sinha and R. K. Mishra. "Control of a nonlinear continuous stirred tank reactor via event triggered sliding modes," *Chemical Engineering Science*, vol. 187, pp. 52–59, Sep. 2018, doi: 10.1016/j.ces.2018.04.057.

[33] D. Li, D. Wang, and Y. Gao. "Adaptive Neural Control and Modeling for Continuous Stirred Tank Reactor with Delays and Full State Constraints," *Complexity*, vol. 2021, p. e9948044, Oct. 2021, doi: 10.1155/2021/9948044.

[34] O. Alshammari, M. N. Mahyuddin, and H. Jerbi. "A Neural Network-Based Adaptive Backstepping Control Law With Covariance Resetting for Asymptotic Output Tracking of a CSTR Plant," *IEEE Access*, vol. 8, pp. 29755–29766, 2020, doi: 10.1109/ACCESS.2020.2972621.

[35] O. Alshammari, M. N. Mahyuddin, and H. Jerbi. "An Advanced PID Based Control Technique With Adaptive Parameter Scheduling for A Nonlinear CSTR Plant," *IEEE Access*, vol. 7, pp. 158085–158094, 2019, doi: 10.1109/ACCESS.2019.2948019.

[36] A. Soukkou, A. Khellaf, S. Leulmi, and K. Boudeghdegh. "Optimal control of a CSTR process," *Braz. J. Chem. Eng.*, vol. 25, pp. 799–812, Dec. 2008, doi: 10.1590/S0104-66322008000400017.

[37] J. Han. "Auto disturbances rejection controller and its applications," *Control Decis.*, vol. 13, no. 1, pp. 19–33, 1998.

[38] Z. Gao, Y. Huang, and J. Han. "An alternative paradigm for control system design," in *Proceedings of the 40th IEEE Conference on Decision and Control (Cat. No.01CH37228)*, Dec. 2001, pp. 4578–4585 vol.5. doi: 10.1109/CDC.2001.980926.

[39] Y. Huang and J. Han. "Analysis and design for the second order nonlinear continuous extended states observer," *Chin.Sci.Bull.*, vol. 45, no. 21, pp. 1938–1944, Nov. 2000, doi: 10.1007/BF02909682.

[40] D. Yoo, S. S.-T. Yau, and Z. Gao. "On convergence of the linear extended state observer," in *2006 IEEE Conference on Computer Aided Control System Design, 2006 IEEE International Conference on Control Applications, 2006 IEEE International Symposium on Intelligent Control*, Oct. 2006, pp. 1645–1650. doi: 10.1109/CACSD-CCA-ISIC.2006.4776888.

[41] X. Yang and Y. Huang. "Capabilities of extended state observer for estimating uncertainties," in *2009 American Control Conference*, Jun. 2009, pp. 3700–3705. doi: 10.1109/ACC.2009.5160642.

[42] B.-Z. Guo and Z. Zhao. "On the convergence of an extended state observer for nonlinear systems with uncertainty," *Systems & Control Letters*, vol. 60, no. 6, pp. 420–430, Jun. 2011, doi: 10.1016/j.sysconle.2011.03.008.

[43] H. Feng and B.-Z. Guo. "Active disturbance rejection control: Old and new results," *Annual Reviews in Control*, vol. 44, pp. 238–248, Jan. 2017, doi: 10.1016/j.arcontrol.2017.05.003.

[44] Z.-H. Wu and B.-Z. Guo. "On convergence of active disturbance rejection control for a class of uncertain stochastic nonlinear systems," *International Journal of Control*, vol. 92, no. 5, pp. 1103–1116, May 2019, doi: 10.1080/00207179.2017.1382720.

[45] Y. Huang, Z. W. Luo, M. Svinin, T. Odashima, and S. Hosoe. "Extended state observer based technique for control of robot systems," in *Proceedings of the 4th World Congress on Intelligent Control and Automation (Cat. No.02EX527)*, Jun. 2002, pp. 2807–2811 vol.4. doi: 10.1109/WCICA.2002.1020036.

[46] Q. Zheng and Z. Gao. "On practical applications of active disturbance rejection control," in *Proceedings of the 29th Chinese Control Conference*, Jul. 2010, pp. 6095–6100. Available: https://ieeexplore.ieee.org/document/5572922.

[47] Q. Zheng, L. Q. Gao, and Z. Gao. "On Validation of Extended State Observer Through Analysis and Experimentation," *Journal of Dynamic Systems, Measurement, and Control*, vol. 134, no. 024505, Jan. 2012, doi: 10.1115/1.4005364.

[48] Q. Zheng and Z. Gao. "Active disturbance rejection control: some recent experimental and industrial case studies," *Control Theory Technol.*, vol. 16, no. 4, pp. 301–313, Nov. 2018, doi: 10.1007/s11768-018-8142-x.

[49] S. E. Talole. "Active disturbance rejection control: Applications in aerospace," *Control Theory Technol.*, vol. 16, no. 4, pp. 314–323, Nov. 2018, doi: 10.1007/s11768-018-8114-1.

[50] E. F. Camacho and C. Bordons, *Model Predictive control*. in Advanced Textbooks in Control and Signal Processing. London: Springer, 2007. doi: 10.1007/978-0-85729-398-5.

[51] A. Isidori, *Nonlinear Control Systems*. in Communications and Control Engineering. London:

Springer, 1995. doi: 10.1007/978-1-84628-615-5.

[52] Z. Gao. "Scaling and bandwidth-parameterization based controller tuning," in *Proceedings of the 2003 American Control Conference, 2003.*, Jun. 2003, pp. 4989–4996. doi: 10.1109/ACC.2003.1242516.